Stanford Exploration Project, Report 115, May 22, 2004, pages 29–38

Short Note

Updating ray-coordinate systems with phase-rays

Jeff Shragge and Biondo Biondi[1]

INTRODUCTION

Riemannian wavefield extrapolation (RWE) casts the problem of wavefield extrapolation in a framework independent of a particular coordinate system (Sava and Fomel, 2003). A practical implementation of RWE, though, requires specifying the computation domain on which to perform extrapolation. One judicious choice is a rayfield where the natural extrapolation direction is stepping in time along an individual ray. Rays in simple media are characterized by smooth curves, and are regularly distributed and (usually) triplication-free. However, rays in more complex media often exhibit tortuous behavior, are irregularly distributed, and are full of triplications. These characteristics, especially triplication, are problematic for the calculation of the derivatives necessary for RWE. Accordingly, a procedure must exist to minimize these adverse effects.

One solution to the ray-coordinate triplication problem is to use velocity models sufficiently smooth such that computed rayfields are triplication-free. The true velocity model is then mapped to the calculated smooth rayfield and RWE is performed as usual. Often, through, the amount of smoothing required to meet this objective causes rays to deviate significant distances from their true ray paths. This spatial relocation leads to a degradation of ray-coordinate extrapolation operator fidelity, because of the non-conformal orientations of the wavefront and extrapolation axes. However, operator accuracy may be partially restored by updating the ray-coordinate system to a basis better aligned with true extrapolation direction. One way to accomplish this is to extrapolate an initial wavefield on an initial ray-coordinate system, and to use this result to calculate a corresponding phase-rayfield (Shragge and Biondi, 2003). This rayfield then forms an improved coordinate basis on which to extrapolate wavefields using RWE.

This short note describes a procedure for updating ray-coordinate systems using phase-rays and RWE. This procedure differs from that of companion paper Shragge and Sava (2004), which presents a recursive bootstrap procedure for calculating a ray-coordinate system on-the-fly using the wavefield phase gradient of the previous few extrapolation steps. This short note is comprised of an overview of the processing flow required to generate the updated phase-rayfield, and examples of the method's application using the Sigsbee 2A velocity model.

[1]**email:** jeff@sep.stanford.edu, biondo@sep.stanford.edu

METHODOLOGY

This section outlines our proposed strategy for updating ray-coordinate systems. This exposition of the required processing steps is intended to be didactic rather than technical. Accordingly, we review in this short note neither the calculation of phase-rays from monochromatic wavefields, nor Riemannian wavefield extrapolation. Instead, we refer the reader interested in the details of either procedure to the more detailed discussions in Shragge and Biondi (2003), Shragge and Sava (2004), and Sava and Fomel (2003).

Calculating an updated coordinate system using phase-ray tracing is a fairly simple procedure involving five processing steps. The goal of this processing is the formation of a coordinate system that better conforms to the orientation of propagating wavefronts. A flow chart of a typical processing sequence is presented in Figure 1. The first step involves developing a

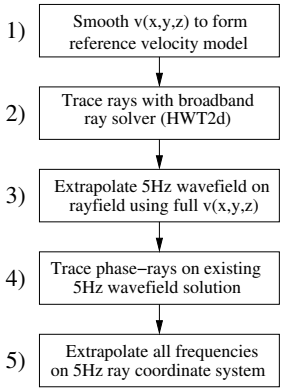

Figure 1: Methodology flow chart illustrating the five processing steps involved in calculating an updated ray-coordinate system in our approach. jeff2-Flow [NR]

velocity model with adequate smoothness such that the corresponding rayfield is triplication-free. To do this, we apply stationary triangular smoothing operators to the true velocity model. The second step is the generation of an initial rayfield using the prepared velocity model. Point source rayfields are modeled by specifying a set of initial ray points located on an arc of some small radius about the shot point. Plane-wave rayfields are generated by seeding rays at all areal acquisition points, and shooting at a constant angle. Planar ray-coordinate systems at different shooting angles are used for extrapolating plane-waves of similar dip. Generally, steps 1 and 2 are repeated until a triplication-free ray-coordinate system is produced.

The third step is to generate an initial monochromatic wavefield solution by: i) performing RWE on the calculated smooth rayfield; and ii) interpolating the resulting wavefield to a Cartesian basis. This step requires mapping a velocity model to the initial ray-coordinate system. Importantly, we are free to choose a velocity function that is not identical to the true model. One strategy is to choose a velocity model that is somewhat rougher than that used to calculate an initial rayfield, but smoother than the exact model. A judicious model choice may yield a wavefield that triplicates, but it should not be too complex to inhibit phase-ray computation.

The fourth step involves using the initial wavefield's phase gradient to calculate an updated ray-coordinate system. This procedure is identical to the calculation of phase-rays discussed in Shragge and Biondi (2003). Attention need be paid to locations where the wavefield magnitude is zero, as they lead to unstable phase-ray calculation. However, because the rayfield only

serves as a proxy for the true wavefront extrapolation direction, we may freely regularize it through application of triangular smoothing operators to generate a smooth ray-coordinate system.

The final step in the procedure comprises: i) a RWE of the broadband wavefield on the updated ray-coordinate system using the true velocity model; ii) and interpolating the resulting wavefield to a Cartesian basis. In principle, steps three and four may be repeated incorporating velocity models of increasing roughness that tend to true velocity model; however, we do not apply this extension here.

EXAMPLE - SIGSBEE 2A

This section presents an example of the ray-coordinate system updating procedure using the Sigsbee 2A velocity model. The velocity model, presented in the lower panel of Figure 2, consists of a typical Gulf of Mexico $v(z)$ velocity gradient overlain by a rugose salt body characterized by significantly higher wavespeed.

The first step of the procedure is shown in the upper panel of Figure 2. The rugosity of the true salt velocity model leads to a plane-wave rayfield containing a substantial number of triplications. To avoid this problem, we iteratively smooth the velocity model with stationary triangular operators. The velocity model shown in the upper panel is the roughest model where rays did not cross. The result of the second step of the procedure, calculating an initial rayfield, is presented in the middle panel. Here, the rays are calculated with a Huygens' wavefront tracing procedure (Sava and Fomel, 2001).

The third step of the procedure is to extrapolate a monochromatic wavefield on the initial rayfield generated in the step 2. This is done using a 5Hz wavefield and the RWE procedure employing the ray-coordinate 15° equation. The resulting wavefield, interpolated to Cartesian coordinates, is shown in the upper panel of Figure 3. The wavefield above and to the left of the salt body is well behaved; however, beneath the top of the salt boundary it exhibits a cross-hatched pattern characteristic of the superposition of different triplication branch phases. This phenomenon is more evident in the sub-salt regions where the lens-like focusing effects of the salt are visible.

The fourth step is to compute the phase-rayfield from the monochromatic wavefield produced in step 3. Results for the 5Hz phase-rayfield are shown in the lower panel of Figure 2. The horizontal extent of the computation grid is less than that of the wavefield in the upper panel, because phase-rays can only be calculated at locations where the initial wavefield was computed. The effects of the rougher velocity model are evident in the shorter wavelength features of the coordinate system. For example, coordinates in the salt body canyons are delayed relative to neighboring points inside the salt body, leading to the sharper corners of the ray-coordinate system below the salt body. Also, the kink in the rayfield in the lower right corner of the lower panel is caused by side boundary reflections masquerading as wavefield triplications. The fifth step of the procedure, calculating a monochromatic wavefield on the updated ray-coordinate system, is illustrated in the lower panel of Figure (3). The resulting

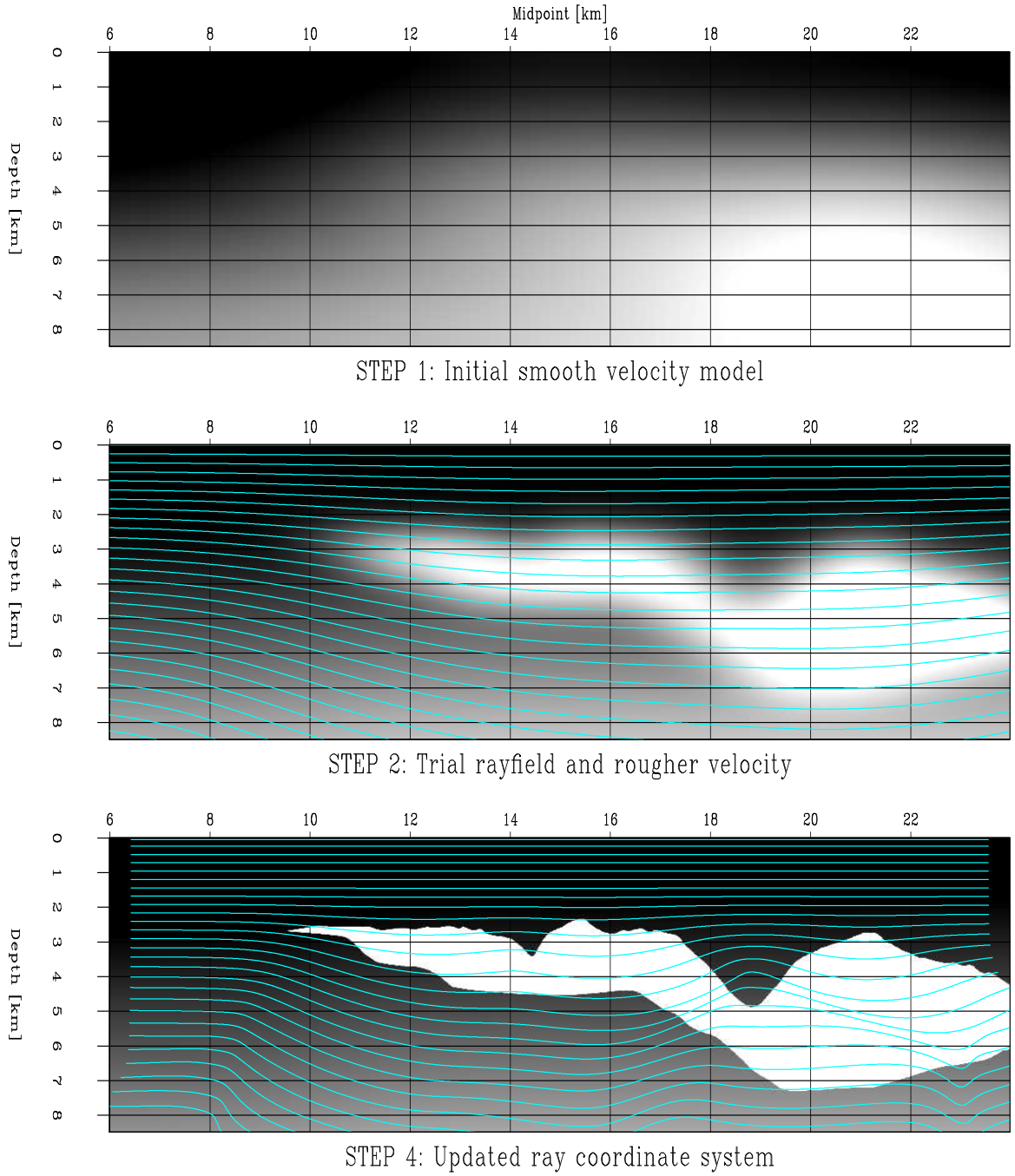

Figure 2: Velocity models and traced rayfields. Upper panel: smoothed Sigsbee 2A velocity model that forms the initial velocity model used for tracing an initial ray-coordinate system. Middle panel: rougher velocity model used for tracing the updated wavefield. The initial ray-coordinate system is overlain; Lower panel: updated 5Hz ray-coordinate system overlying the unsmoothed Sigsbee 2A velocity model. jeff2-Ziggy.raycomparison [CR]

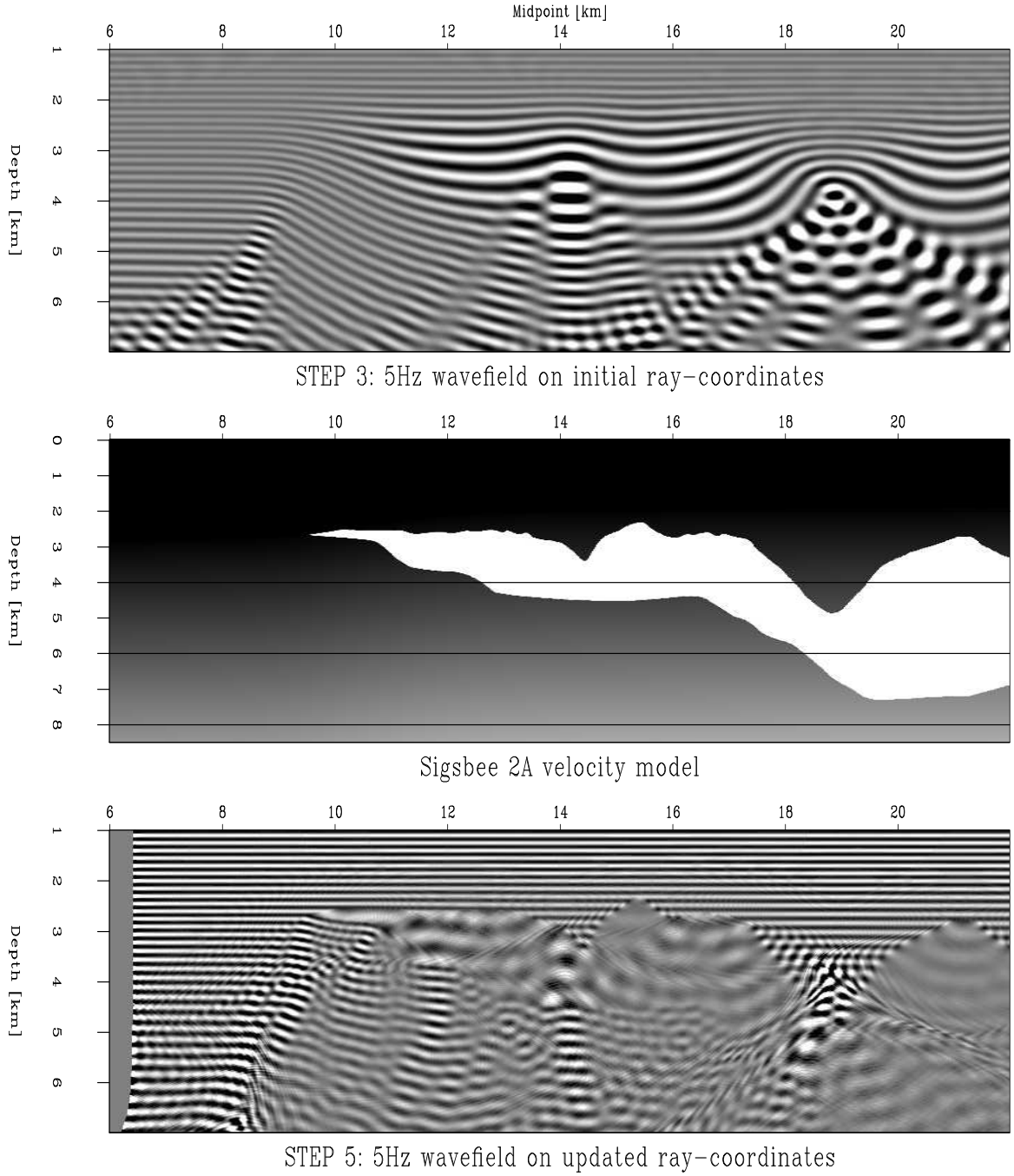

Figure 3: Calculated monochromatic 5Hz wavefields. Upper panel: initial wavefield solution calculated on initial ray-coordinate system using the rougher velocity model; Middle panel: Sigsbee 2A velocity model; Lower panel: updated wavefield solution calculated on updated ray-coordinate system. jeff2-Ziggy.raysoln [CR]

wavefield is full of triplications, and the illumination gaps (areas of low wavefield intensity) observed by Clapp (2003) are now plainly visible.

Broadband wavefields computed on the initial and updated ray-coordinate systems are presented in the upper panels of Figure 4. For interest, we include the velocity model mapped into both of these coordinate systems (lower panels). The horizontal lines represent surfaces of constant extrapolation time. The upper panels show the initial plane-wave after propagation from the surface to depth through the respective velocity models. Results are presented at three travel-time steps spaced out at one second intervals. If the coordinate system were perfect, extrapolated wavefronts would be collinear with the three straight lines. This would indicate that the wavefront remains perfectly conformal with the ray-coordinate system. (Diffracted energy, though, moves sub-parallel to the wavefront and therefore does not form a straight line).

Differences in wavefront curvature between the upper two panels illustrate that the angles formed between the wavefront and extrapolation axes have, indeed, changed. In particular, they are now greater on the left side than on the right, which is not surprising because our goal is creating a coordinate system more conformal with the wavefront orientation. (Recall that a decreased extrapolation angle corresponds to increased operator fidelity.) This improved alignment, though, does come at a cost: the flanks of the canyon between 17 and 20km in midpoint are now steeper than in the original velocity model. This means that extrapolation across the salt flanks is now less robust because the salt flank angles are too severe. A result of this problem is observable in the less realistic extrapolated wavefield in the salt canyon between 2-3s in time and 17 and 20km in midpoint.

From this example, we point out that the ability to create a ray-coordinate system actually leads to an extra degree of freedom in the extrapolation process. As a result, the practitioner must resolve the trade-off between how well a wavefront conforms with the ray-coordinate system and how steep the structural dips of the velocity model are mapped as a result. Thus, one must ask the question: is it better to account for the steepest structural dips in the velocity model, but with lower extrapolation accuracy? or is it better to handle only shallower structural dips but with greater accuracy? Our conjecture is that the answer lies somewhere between these two end members and strongly depends on the particular velocity model in question.

The wavefields of Figure 4, interpolated to a Cartesian basis, are presented in Figure 5. The upper and lower panels present the broadband extrapolation results computed using the initial and updated ray-coordinate systems, respectively. Snapshots of the wavefields at the first depth level is fairly similar; however, the second and third are markedly different. The wavefield in the lower panel at the fourth snapshot is more continuous across the breadth of the computational grid. However, beneath the salt canyon described above, the extrapolated wavefields in the upper panel seem to be more representative of the expected propagation results. This lack of global improvement is an example of the trade-off discussed above.

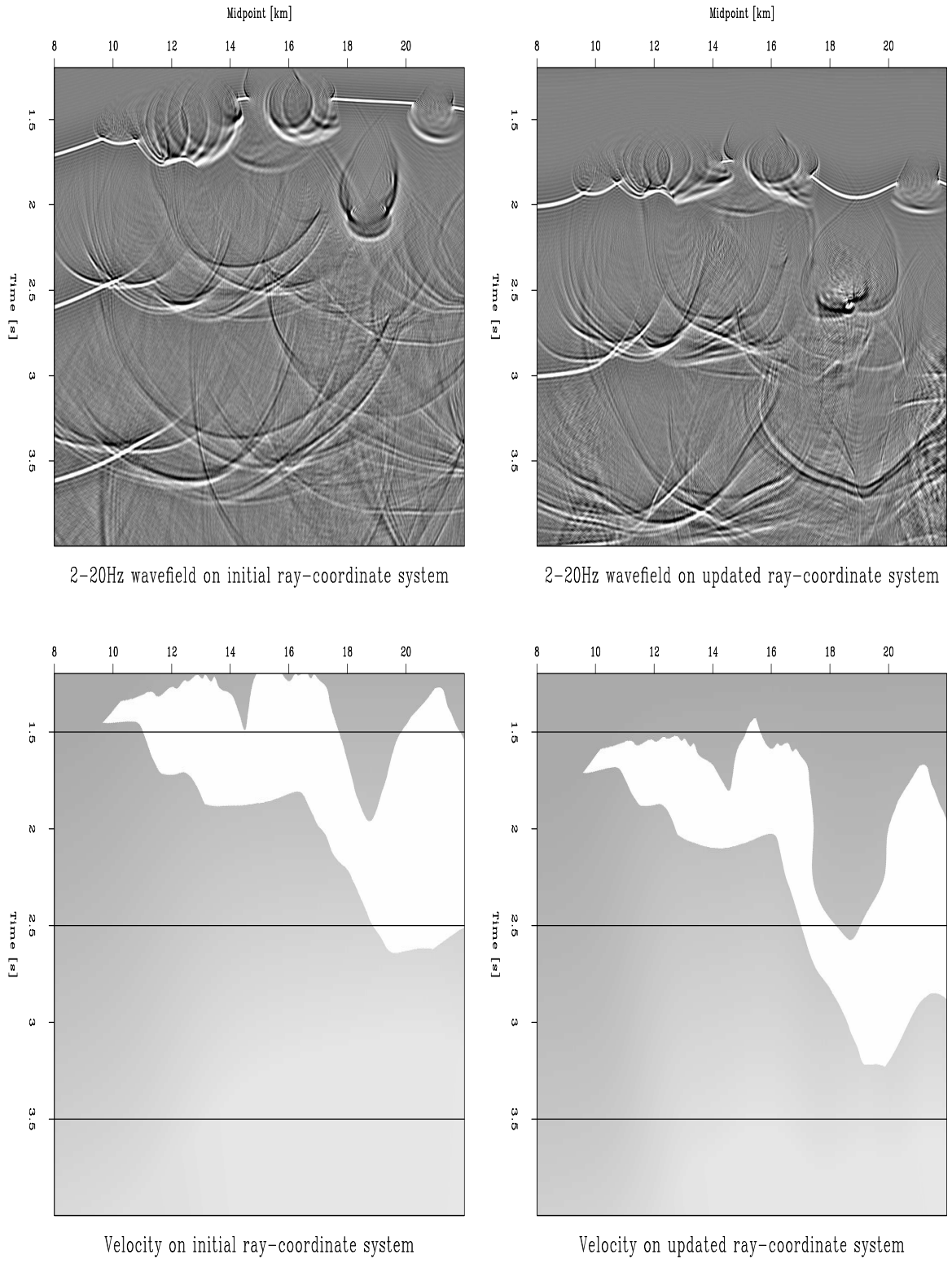

Figure 4: Calculated broadband wavefield solutions in ray-coordinates (2-20Hz). Upper left panel: wavefield computed on initial ray-coordinate system; Upper right panel: wavefield computed on updated ray-coordinate system; Lower left panel: velocity model mapped to the initial ray-coordinate system; Lower right panel: velocity model mapped to the updated ray-coordinate system. jeff2-Ziggy.allraysoln [CR]

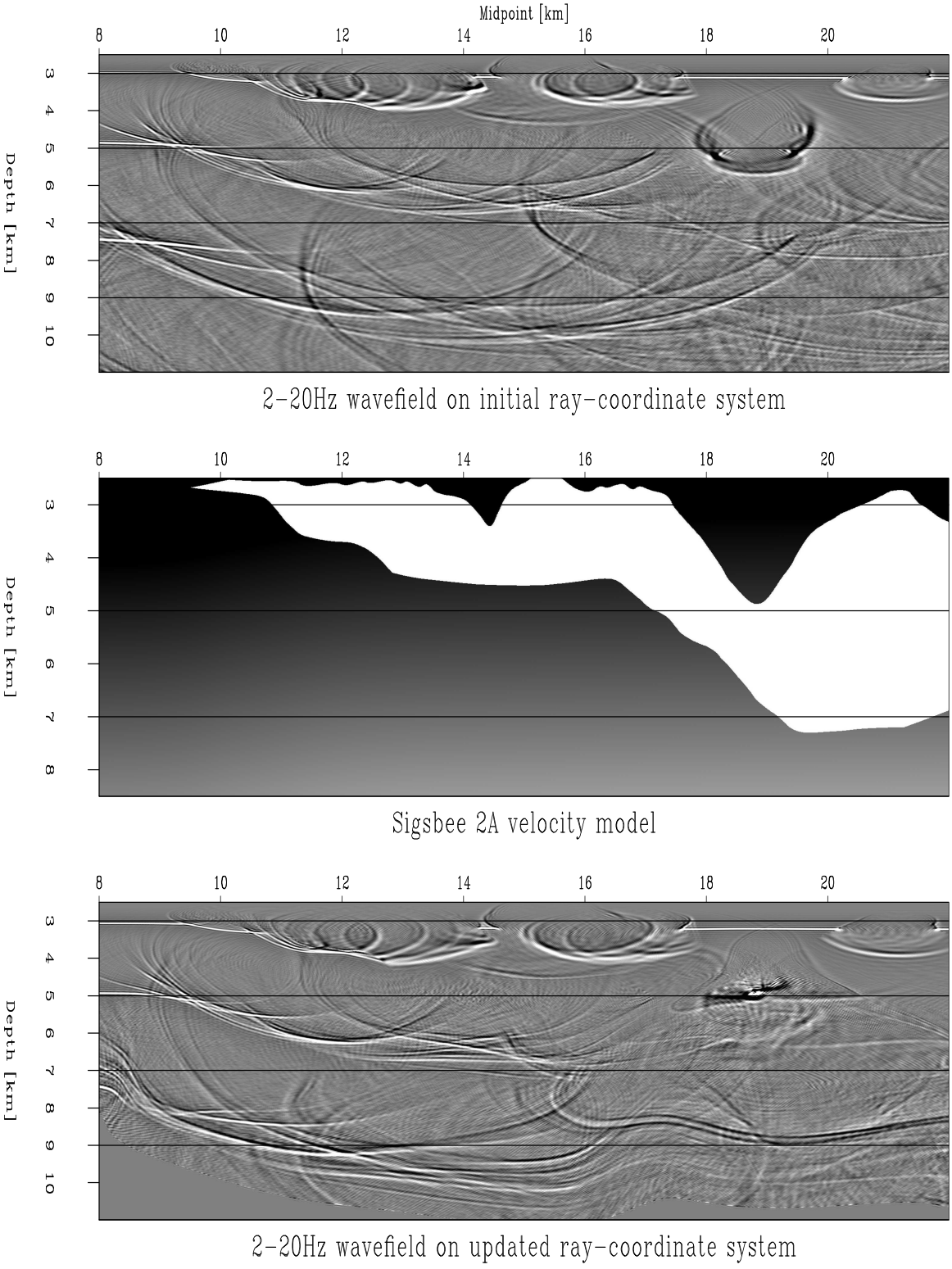

Figure 5: Calculated broadband wavefield solutions in Cartesian coordinates (2-25Hz). Upper panel: wavefield calculated on initial ray-coordinate system; Middle panel: Sigsbee 2A velocity model; lower panel: wavefield calculated on a updated ray-coordinate system. jeff2-Ziggy.allcartsoln [CR]

CONCLUSIONS

We present a procedure for calculating ray-coordinate system updates incorporating RWE and phase-ray tracing. This procedure can successfully generate a ray-coordinate systems that better conforms with the direction of wavefield propagation. This fact then leads to an improved wavefield extrapolation operator fidelity. However, coordinate system realignment is not always a global advantage. This is because, as a result, structural dips may be mapped more steeply in the updated ray-coordinate velocity models. Importantly, steeper structural dip angles in the velocity model also inhibit the accuracy of wavefield extrapolation. Accordingly, we suggest that a trial-and-error (or a more sophisticated) approach could be used to generate a ray-coordinate system for RWE that represents an optimal trade-off between improving operator fidelity and lowering structural dips in resulting velocity models.

ACKNOWLEDGMENTS

We acknowledge Western Geco for permission to use the Gulf of Mexico velocity model. We also thank Paul Sava and Antoine Guitton for helpful discussions.

REFERENCES

Clapp, M. L., 2003, Velocity sensitivity of subsalt imaging through regularized inversion: SEP–**114**, 57–66.

Sava, P., and Fomel, S., 2001, 3-D traveltime computation by Huygens wavefront tracing: Geophysics, **66**, no. 3, 883–889.

Sava, P., and Fomel, S., 2003, Seismic imaging using Riemannian wavefield extrapolation: SEP–**114**, 1–30.

Shragge, J., and Biondi, B., 2003, Wavefield extrapolation in phase-ray coordinates: SEP–**114**, 31–44.

Shragge, J., and Sava, P., 2004, Adaptive phase-ray wavefield extrapolation: SEP–**115**, 13–28.